RSC Advances

ROYAL SOCIETY OF CHEMISTRY

PAPER

View Article Online
View Journal | View Issue

Cite this: *RSC Adv.*, 2026, **16**, 1068

Zinc molybdenum thiovanadate nanoparticles: synthesis, characterization, and antibacterial activity

Fatimah Alahmari *

Infection control is a key point for maintaining and developing the healthcare sector. Nanosized metal derivatives have attracted significant interest for preventing infections caused by various bacteria and fungi. This study reports the synthesis of new sulfide nanoparticles containing bioactive Zn, Mo, and V in one structure. Powder X-ray diffraction (PXRD) analysis was used to determine the structure, phase purity, and crystallite size of the $ZnMoVS_4$ nanoparticles (NPs). The results reveal the presence of only one phase corresponding to a cubic close-packed spinel structure in the $F\bar{4}3m$ (216) space group. The calculated crystallite (grain) size is 16.86 nm, which falls within the nanoparticle size range. High-resolution transmission electron microscopy (HR-TEM) was utilized to verify the nanoscale size and crystallinity of the NPs and to examine their morphology. High-angle annular dark-field scanning transmission electron microscopy (HAADF-STEM) was used to perform elemental mapping and confirm the chemical composition of the prepared NPs. X-ray photoelectron spectroscopy (XPS) analysis was performed to confirm the presence and oxidation states of all the introduced elements. These results are consistent with the proposed chemical formula of $ZnMoVS_4$ for the prepared NPs. The bioactivity of the prepared NPs was studied using three waterborne Gram-negative bacteria: *Escherichia coli*, *Salmonella choleraesuis*, and *Shigella flexneri*. The results revealed the significant effect of the $ZnMoVS_4$ NPs on the studied bacteria. However, *Escherichia coli* showed greater suppression upon treatment than *Salmonella choleraesuis* and *Shigella flexneri*. Hence, the introduced NPs are promising antimicrobial candidates for water treatment to prevent waterborne bacterial diseases.

Received 17th September 2025
Accepted 18th December 2025

DOI: 10.1039/d5ra07046e

rsc.li/rsc-advances

Introduction

Nanotechnology is playing a significant role in current breakthroughs in the environmental, industrial, and medical sectors. The unique physical and chemical properties of materials at the nanoscale make them a central topic for research in chemistry and materials science. Nanomaterials are lighter in weight, smaller in size, have a larger surface area, and exhibit greater reactivity than the same material in bulk.[1]

Metal sulfide nanomaterials have attracted considerable interest due to their wide range of applications in diverse fields. These materials are composed of metal cations bonded to sulfur atoms in a variety of configurations. As a result, they exhibit distinctive optical, electrical, and catalytic properties that offer several advantages over their metal oxide counterparts.[2] Metal sulfide nanomaterials have been applied in diverse fields, such as electronics, energy storage, catalysis, and sensing.[2–4] The tunable properties and high reactivity of these materials have extended their utilization in fields ranging from environmental remediation to biomedical applications.[5,6]

In biomedicine, metal sulfide nanomaterials hold significant potential for advancing diagnostics, imaging, and therapy.[7] Moreover, the tunable surface chemistry and biocompatibility of many metal sulfide nanomaterials enable their functionalization as targeted drug delivery systems.[8]

Zinc sulfide (ZnS) is one of the most investigated metal sulfides for biomedical applications at the nanoscale owing to its biocompatibility, low toxicity and unique physicochemical properties at the nanoscale.[9] As expected, ZnS nanoparticles have demonstrated excellent antimicrobial activity against a broad spectrum of bacterial strains, making them potential candidates for combating infections.[10,11] For drug delivery, nanosized ZnS particles can be functionalized to act as carriers for therapeutic agents, enabling controlled release and precise targeting of specific cells or tissues.[12] Moreover, the luminescence property of nanosized ZnS allows *in vitro* imaging of targeted cancer cells during treatment.[13]

Molybdenum sulfide (MoS_2) nanosheets (NSs) are a remarkable class of two-dimensional materials with exceptional properties. These NSs are typically composed of a single or a few layers of molybdenum disulfide.[14] The unique structure of these materials, which resembles that of graphene but with distinct

Department of Nanomedicine Research, Institute for Research and Medical Consultations (IRMC), Imam Abdulrahman Bin Faisal University, P. O. Box 1982, 31441, Dammam, Saudi Arabia. E-mail: fsalahmari@iau.edu.sa

electronic and chemical characteristics, makes them ideal for use in various fields.[14–16] In biomedicine, MoS_2 NSs have attracted significant interest because of their distinctive properties, such as adjustable optical properties, excellent electrochemical properties, high surface area, biocompatibility, low toxicity and catalytic activity.[15–17] For drug delivery, MoS_2 NSs can be used to effectively load and release therapeutic agents, offering controlled drug delivery with minimal side effects.[18,19] Moreover, its excellent photothermal properties enable it to serve as a robust agent for photothermal therapy.[19–21] MoS_2 NSs have also played a role in improving imaging techniques, including photoacoustic and fluorescence imaging, by offering high-resolution imaging capabilities that support more accurate diagnosis and treatment planning.[22,23]

Vanadium sulfide (V_xS_y) nanomaterials have various formulas and morphologies due to the multiple oxidation states of V (V^{2+}–V^{5+}).[24,25] Although these materials are well investigated for industrial purposes, their biocompatibility, high surface area and tunable characteristics allow for the functionalization needed for various bioapplications.[26] Moreover, they contain vanadium, which plays an important role in many biological applications, including drug delivery, antimicrobial treatment, biosensing, imaging and treating several diseases as a therapeutic agent.[27–29] A recent study reported the efficacy of vanadium disulfide (VS_2) NSs in cancer immunotherapy and immune checkpoint blockade therapy.[26]

For the health care, food processing and water purification fields, combating bacterial infection is essential. Bacteria can develop resistance to common antibacterial treatments, which occurs when bacteria evolve mechanisms to withstand the effects of those antibiotics. The main reason is the overuse and misuse of antibiotics in healthcare and agriculture.[30–32] Thus, innovative solutions are needed to overcome this issue, including the promotion of responsible antibiotic use and the development of new antibacterial agents.[33]

Usually, increasing the complexity of nanostructures enhances their bioactivity by introducing multifunctionality, precise targeting, and improved interactions at the cellular level.[34]

The combination of bioactive Zn, Mo, and V within a single sulfide structure is anticipated to enhance its antibacterial activity through synergistic effects. Zn ion is well-known for its antimicrobial activity and role in promoting cellular repair.[10,11] Mo ions influence oxidative processes and contribute to reactive oxygen species (ROS) generation, leading to oxidative stress in bacterial cells.[35,36] V ions demonstrated strong antibacterial potential due to their redox versatility and ability to accelerate electron transfer reactions that promote ROS formation.[37,38]

Integrating these components in one sulfide lattice may therefore yield a multifunctional nanomaterial with enhanced antibacterial efficiency through combined oxidative and membrane-disruptive actions. This constructive interaction provides a rational basis for exploring such nanostructures as promising bioactive agents for infection control and waterborne pathogen management.

Herein, the synthesis of $ZnMoVS_4$ nanoparticles (NPs) is reported for the first time *via* a one-pot solvothermal reaction using thiourea. The antibacterial activity of the synthesized NPs was determined against selected waterborne bacterial pathogens.

Experimental

Instrumentation

This study utilized various characterization techniques to analyze the synthesized NPs. Powder X-ray diffraction (PXRD) analysis was carried out using a Rigaku Benchtop Miniflex diffractometer equipped with a Cu Kα radiation source ($\lambda = 1.5406$ Å). The measurements were performed at 40 kV and 15 mA under ambient conditions. Diffraction patterns were recorded in the 2θ range of 20–80° with a step size of 0.05° and a scan rate of 2° min^{-1}. The obtained diffraction data were analyzed using PDXL2 software for phase identification by comparison with standard reference patterns from the ICDD database. The PXRD results confirmed the crystalline nature and phase purity of the synthesized NPs. Transmission electron microscopy (TEM) and selected area electron diffraction (SAED) analysis were performed with a Thermo Fisher Scientific Titan Themis Z equipped with a double Cs corrector, a high-brightness electron gun (x-FEG), and an electron beam monochromator. The TEM analysis was carried out by operating the microscope at the accelerating voltage of 300 kV and with a beam current of 0.5 nA. The Dark field imaging was performed by scanning TEM (STEM) coupled to a high-angle annular dark-field (HAADF) detector. The STEM-HAADF data were acquired with a convergence angle of 20.9 mrad. Furthermore, an X-ray energy dispersive spectrometer (SuperX) was also utilized in conjunction with DF-STEM imaging to acquire STEM-EDS spectrum-imaging data sets. The processing of HRTEM images and SAED patterns was made with the Gatan software GMS3 and the process of EDX maps was done using Velox Thermo Fisher software. The elemental mapping technique, integrated with HR-TEM analysis, enabled the identification and spatial distribution of all the elements forming the NPs. Additionally, X-ray photoelectron spectroscopy (XPS) analysis was performed using a Kratos Axis Ultra spectrometer equipped with a monochromatic Al Kα X-ray source ($h\nu = 1486.6$ eV). The measurements were carried out under ultrahigh vacuum conditions ($\sim 1 \times 10^{-9}$ mbar) with a pass energy of 20 eV for high-resolution scans and 160 eV for survey spectra. The binding energy scale was calibrated using the C 1s peak at 284.8 eV as a reference. Data processing and peak fitting were performed using ESCApe software, employing a Shirley background and Gaussian–Lorentzian peak shapes. The obtained spectra provided detailed information on the elemental states, the chemical composition, and the surface characteristics of the NPs.

NPs synthesis

$ZnMoVS_4$ NPs were synthesized through a solvothermal reaction using metal precursors, thiourea for sulfurization, and ethanol as the solvent. Oxalic acid was used as a reducing agent, while polyvinylpyrrolidone, 1 300 000 molecular wight (PVP1300000) was incorporated as a growth modifier and dispersant to stabilize and control the shape of the NPs and reduce their size.[39,40]

The successful synthesis of $ZnMoVS_4$ NPs was out of a systematic study and more than twenty reactions were conducted to find the best conditions for producing a pure phase of these NPs.

The study included using different metal precursors such as VCl_3, $Na_2MoO_4 \cdot 2H_2O$, and different sulfur sources such as sulfur powder (S_8) and thiourea, while the solvent was fixed to be ethanol for all reactions. For the reducing agent and stabilizer, reactions were carried out with and without oxalic acid, with and without PVP and without both. The reactions were performed under three heating profiles: 150 °C, 180 °C and 200 °C. The reaction and conditions producing the reported $ZnMoVS_4$ NPs was repeated five times to check the reproducibility and each time a pure phase of the NPs was formed (confirmed by PXRD). Following is the detailed description for $ZnMoVS_4$ NPs synthesis under the best conditions.

The procedure started by mixing 2 mmol of each NH_4VO_3 (0.234 g) and $Zn(CH_3COO)_2 \cdot 2H_2O$ (0.44 g) and 0.28 mmol of $(NH_4)_6Mo_7O_{24} \cdot 4H_2O$ (0.353 g) with 140 mL of absolute ethanol in a 200 mL Teflon-lined vessel. Then, 40 mmol (3 g) of thiourea, 20 mmol (1.8 g) of anhydrous oxalic acid and 0.0015 mmol (2 g) of PVP1300000 were added to the mixture and kept stirring magnetically for 2 hours. The vessel was then closed and sealed in a stainless-steel autoclave and heated in a preheated oven at 200 °C for 48 hours. After cooling, the vessel was unsealed, and a grey colloidal solution had formed. The dark gray precipitate of the NPs was collected by centrifugation and washed with absolute ethanol six times until the solution was clear. The product was dried using diethyl ether and subsequently kept in a vacuum oven at 80 °C overnight. The final yield of the NPs was 0.52 g (±0.05), ~96% indicating that the metal precursors are fully reacted under the given conditions.

Antibacterial activity

The commercially available Gram-negative bacterial strains *S. choleraesuis* (ATCC10708), *S. flexneri* (ATCC12022) and *E. coli* (ATCC352118) were chosen to evaluate the antibacterial action of the synthesized $ZnMoVS_4$ NPs. The fresh inoculum was prepared by inoculating a pure colony in nutrient broth (MOLEQULE-ON, cat no: MM-M-060-500) and incubating in an incubator shaker at 110 rpm and 37 °C overnight. Later, the bacterial cells obtained were washed with phosphate-buffered saline (PBS) and adjusted with 0.9% NaCl solution to obtain a concentration of 10^6 CFU mL^{-1} as a standardized inoculum.

The macro broth dilution technique was used to evaluate the MIC/MBC of the $ZnMoVS_4$ NPs against the test bacteria. The bacterial suspension was prepared in sterile Mueller–Hinton broth (Scharlau 02-136-500), along with synthesized and sonicated $ZnMoVS_4$ NPs at concentrations ranging from 0.25 mg mL^{-1} to 16 mg mL^{-1} for each bacterium and further incubated. The growth control (without $ZnMoVS_4$ NPs) and media control were included and incubated in an incubator shaker according to the above-described parameters. The MIC offers the minimum concentration of $ZnMoVS_4$ NPs that suppresses bacterial growth. Subsequently, after evaluation of the MIC, aliquots of treated bacteria were inoculated on fresh sterile MHA plates. The lowest concentration of $ZnMoVS_4$ NPs that caused no growth or colony formation in fewer than three cells was recorded as the MBC.[41] The experiments were repeated twice for reliability and the findings were the same each time.

Results and discussion

The prepared $ZnMoVS_4$ NPs have been the subject of structural and morphological investigations utilizing a variety of methods, such as PXRD, HR-TEM, HAADF-STEM and XPS. Understanding the crystal structure, shape and composition is crucial for evaluating nanomaterials characteristics promoting their bioactivity examination.

Structure and morphology

Fig. 1 shows the Rietveld refined PXRD pattern for the $ZnMoVS_4$ NPs. The plot indicates the existence of a single-crystalline phase, which is consistent with a cubic close-packed spinel structure in the $F\bar{4}3m$ (216) space group.[42] From the structure refinement, the lattice constant a is equal to 5.393 Å.[43] The crystallite (grain) size corresponding to the highest intensity peak related to the (111) plane was calculated using the Scherrer equation to be 16.86 nm.[44]

The prepared NP samples were studied by high resolutions TEM (HR-TEM) imaging to confirm their nanosize and crystallinity. Fig. 2 displays HR-TEM images captured at different resolutions, which show aggregations of particles with an average size ≥20 nm. The observed aggregation can be attributed primarily to their high surface energy and strong van der Waals and interactions. Such aggregation can occur during the solvent evaporation and drying process used in TEM grid preparation. While aggregation may reduce the effective surface area accessible for antibacterial interactions, it can also enhance structural stability and facilitate electron transport between adjacent nanoparticles. These interparticle contacts can promote charge carrier mobility and improve redox activity, which are beneficial for antibacterial performance.[45]

The integration of the lattice fringes at 2 nm (Fig. 2d) gave two values of d-spacing, $d_{(111)} = 0.318$ nm and $d_{(200)} = 0.282$ nm, corresponding to the (111) and (200) planes, respectively.

In Fig. 2e, the selected area electron diffraction (SAED) pattern at a specific spot shows a well-defined diffraction

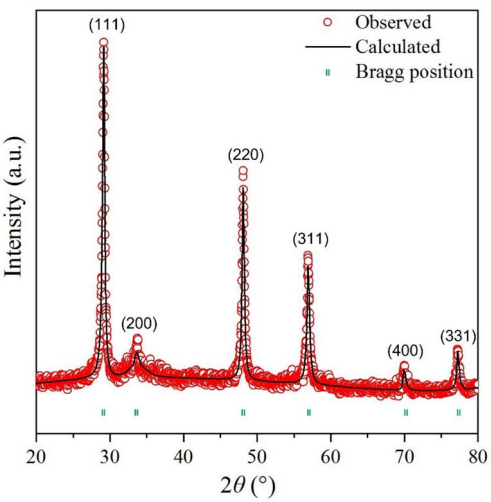

Fig. 1 Rietveld refined PXRD pattern for $ZnMoVS_4$ NPs.

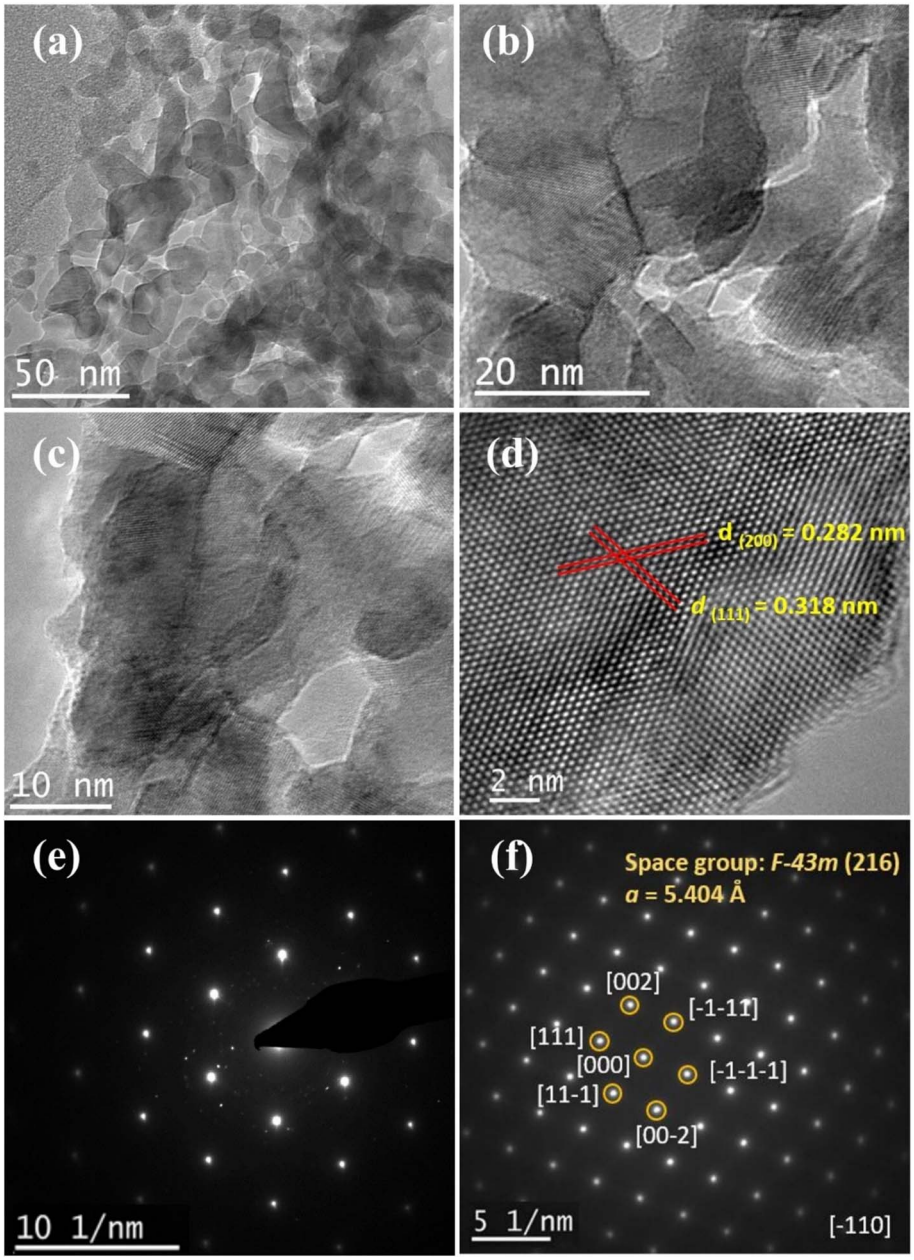

Fig. 2 HR-TEM images (a) at 50 nm, (b) at 20 nm, (c) at 10 nm, and (d) at 2 nm showing lattice fringes; (e and f) SAED analysis and peak indexing.

pattern reflecting the high crystallinity of the sample. The indexing planes in the SAED pattern (Fig. 2f) match the space group $F\bar{4}3m$ (216) with a lattice constant a of 5.404 Å. The lattice constant derived from PXRD refinement (5.393 Å) showed a minor deviation from that obtained through SAED (5.404 Å). This slight difference can be attributed to variations in measurement principles and calibration accuracy between the two techniques. PXRD represents an average over the entire crystalline sample, whereas SAED is a localized probe that may reflect subtle lattice distortions or strain in individual nanoparticles. The observed variation (~0.01 Å) falls within the expected experimental tolerance for nanoscale materials and confirms good consistency between the two analyses.

The integration of the lattice fringes at 2 nm (Fig. 2d) gave two values of d-spacing, $d_{(111)} = 0.318$ nm and $d_{(200)} = 0.282$ nm, corresponding to the (111) and (200) planes, respectively. Elemental mapping was performed using HAADF-STEM coupled with EDX to confirm the chemical composition of the $ZnMoVS_4$ NPs (Fig. 3). All the elements in the proposed formula appear in the examined sample. EDX elemental mapping confirms a homogeneous distribution of Zn, Mo, V, and S throughout the $ZnMoVS_4$ nanostructure. The measured atomic ratio of Zn : Mo : V : S is approximately 1 : 1 : 1 : 4, based on semi-quantitative EDX analysis of three representative regions, with standard deviations of ±0.03, ±0.05, ±0.05, and ±0.10, respectively.

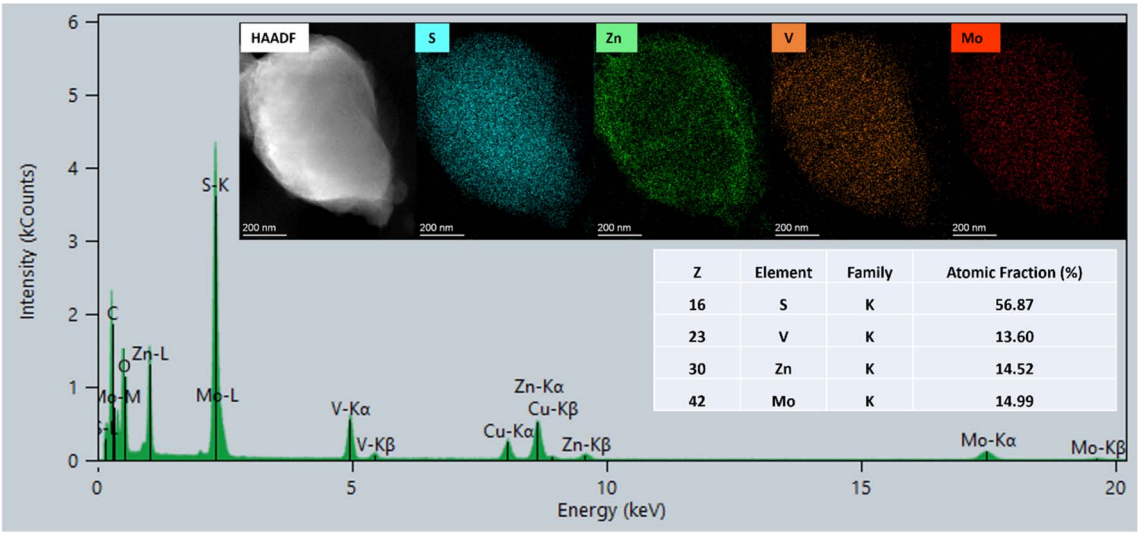

Fig. 3 HAADF-STEM elemental mapping of $ZnMoVS_4$ NPs.

Fig. 4 shows the XPS analysis of the $ZnMoVS_4$ NPs performed to determine the presence and oxidation states of all the elements aligning with the chemical formula. A survey scan was performed to detect all the elements in the sample, which confirmed the presence of Zn, Mo, V and S.

The S 2p narrow spectrum shows two overlapping peaks at 161.5 eV and 162.2 eV according to the $2p_{3/2}$ and $2p_{1/2}$ spins, respectively, characteristic of S^{2-} in sulfide species.[46–48]

The S 2s peak overlaps with the Mo 3d spectrum and appears at 225.1 eV, while the Mo 3d peaks split over 229.2 for Mo $3d_{5/2}$ and 232.3 for Mo $3d_{3/2}$. These values are typically attributed to Mo^{3+} in sulfide environments, which are consistent with the reported values for Mo^{3+} in $CoMo_2S_4$.[49] Although Mo^{3+} is less common in sulfides compared to Mo^{4+} (*e.g.*, in MoS_2), Mo^{3+} species can be stabilized in sulfide systems under sulfide-rich or reducing conditions such as in Mo_2S_3 and $CoMo_2S_4$.[49,50]

The Mo 3p XPS spectrum displays two peaks at 396.2 and 412.2 eV related to Mo $2p_{3/2}$ and Mo $2p_{1/2}$, respectively, for the core level of Mo^{3+}.[51]

The V 2p XPS spectrum shows two peaks at 513.3 and 520.6 eV associated with V^{3+} spins, V $2p_{3/2}$ and V $2p_{1/2}$, respectively.[52,53] These values are consistent with the V^{3+} 2p reported values in sulfides such as ZnV_2S_4 and Cu doped CoV_2S_4.[54,55]

The Zn 2p XPS spectrum exhibits two distinct sharp peaks at 1042.1 eV and 1018.9.2 eV belong to Zn $2p_{3/2}$ and Zn $2p_{1/2}$, respectively, for the Zn^{2+} oxidation state.[48,56] XPS analysis verified the purity and chemical composition of the synthesized NPs, identified as $Zn^{2+}V^{3+}Mo^{3+}S_4$. This result is supported by the PXRD analysis which confirmed that the prepared NPs adapts the thiospinel structure and EDX elemental mapping results.

Antibacterial activity

Fig. 5 displays the antibacterial activity study for $ZnMoVS_4$ NPs against *S. choleraesuis*, *S. flexneri* and *E. coli* by evaluating the MIC and MBC *via* the broth dilution method. For *S. choleraesuis* and *S. flexneri*, the lowest effective MIC/MBC concentration for the $ZnMoVS_4$ NPs is 4 mg mL; however, for *E. coli*, the lowest effective MIC/MBC concentration is 1 mg mL^{-1} of the $ZnMoVS_4$ NPs. As shown in Fig. 5, *E. coli* was the most affected bacterium compared with the other two Gram-negative organisms. The difference in action among all the three Gram-negative organisms could be attributed to the effective interaction/attachment of NPs to the specific cell wall receptors of each bacterium. The results revealed the variation in the antibacterial inhibition of Gram-negative bacteria treated with $ZnMoVS_4$ NPs compared to that of the control bacteria, which were not treated but were grown under similar experimental conditions. Overall, the $ZnMoVS_4$ NPs inhibited the growth of all the tested Gram-negative bacteria, which are mostly responsible bacteria for waterborne diseases. However, *E. coli* showed greater suppression upon treatment than *S. cholerasuis* and *S. flexneri*.

The obtained antibacterial activities of $ZnMoVS_4$ NPs can be correlated to the multi-elemental nature that imparts the multi-mechanistic action against the tested bacteria. It has already been reported that zinc ions in nanostructures tend to exert significant antimicrobial activity through a number of mechanisms of mechanisms as membrane distortion, metal and cellular protein interactions, and reactive oxygen species (ROS) generation.[10,11] Molybdenum and vanadium ions are also known for their strong catalytic and redox potential and electron transfer acceleration, promoting the generation of ROS and thereby inducing the oxidative stress in bacterial cells.[35–38] The integration of sulfur additionally enhances the interactions with thiol possessing membrane proteins, promoting permeability of the bacterial membrane.[57] Such combined mechanisms are commonly have a synergistic impact, resulting in effective antibacterial action compared to individual metals or metal oxides NPs.

Silver nanoparticles (Ag NPs) are extensively studied as potent antibacterial agents owing to their ability to release Ag^+ ions and enhance the ROS generation.[58,59] $ZnMoVS_4$ NPs exhibited comparable antibacterial activity to Ag NPs against

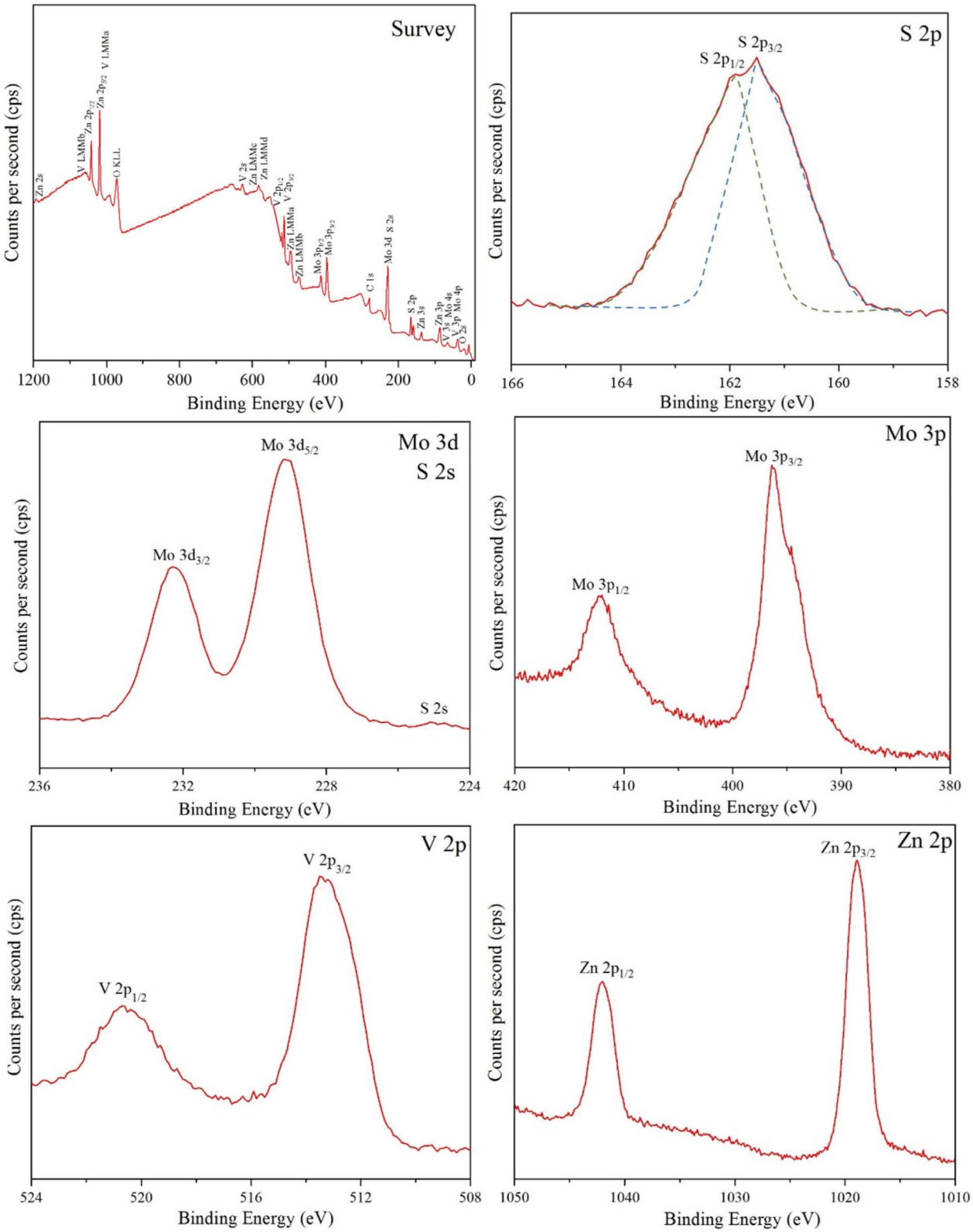

Fig. 4 XPS analysis of $ZnMoVS_4$ NPs.

the tested strain. On the contrary, Ag NPs are associated with toxicity and environmental hazards.[58,60] The synthesized $ZnMoVS_4$ NPs may possess advantages over Ag NPs, *e.g.*, synergistic redox potential reactions *via* physiochemical active metal ions attributed to the anionic sulfide matrix, and biocompatibility (based on components). The outcome of the

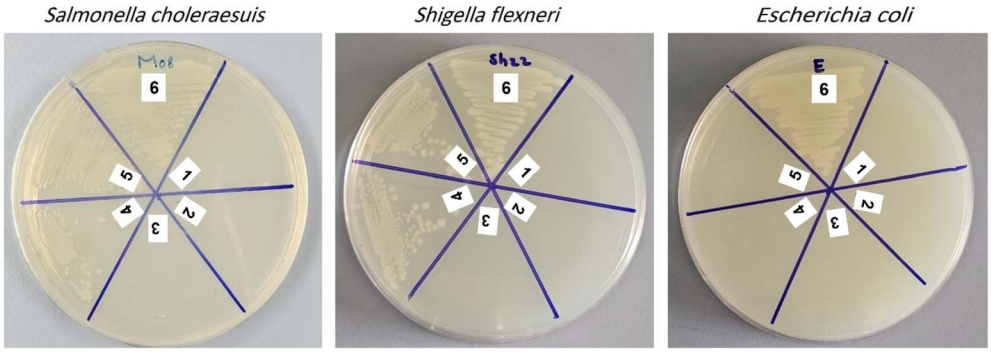

Fig. 5 MHA agar plates showing the MIC/MBC of *S. choleraesuis*, *S. flexneri* and *E. coli* upon treatment with $ZnMoVS_4$ NPs (1: 16 mg mL^{-1}, 2: 8 mg mL^{-1}, 3: 4 mg mL^{-1}, 4: 2 mg mL^{-1}, 5: 1 mg mL^{-1}, 6: untreated bacteria).

current study aligns with earlier reports supporting that multimetallic NPs usually perform better than monometallic NPs because of the combined redox and mechanisms related to membrane interactions.[61,62] For $ZnMoVS_4$ NPs, the combination of bioactive Zn, Mo, and V within a single sulfide structure is anticipated to enhance its antibacterial activity through synergistic effects. Integrating these components in one sulfide lattice may therefore yield a multifunctional nanomaterial with enhanced antibacterial efficiency through combined oxidative and membrane-disruptive actions. These characteristics potentially contribute to the improved antibacterial activity observed in the current study.

Moreover, the size and morphology of the NPs can contribute significantly to the antibacterial potential. Smaller sized NPs with increased crystallinity possess greater surface/volume ratios, encouraging maximum interaction with cellular membranes/walls and enhanced ROS generation.[63] Furthermore, as confirmed by EDX analysis, the uniform distribution of elements proves that each nanoparticle bears a consistent ratio of zinc, molybdenum, vanadium, and sulfur, which is also responsible for the obtained antibacterial effects. Although the HR-TEM images (Fig. 2) show some aggregation which may reduce the effective surface area accessible for antibacterial interactions, it does not compromise and may even enhance the overall antibacterial functionality of $ZnMoVS_4$ NPs. In fact, the interparticle contacts can promote charge carrier mobility and improve redox activity, which are beneficial for antibacterial performance through the generation of reactive oxygen species (ROS).[45]

The present study demonstrates that $ZnMoVS_4$ NPs are impactful and possess a wide range of mechanistic ways for imparting the antimicrobial effect. Such a finding has important relevance in the current global issue of antimicrobial resistance (AMR). Bioactive NPs that work through multiple actions like membrane disruption, oxidative stress, and metabolic interference minimize the chance of developing resistance, compared to conventional antimicrobials that acts on specific proteins.[64] Thus, $ZnMoVS_4$ NPs may represent a potential candidate for upcoming antimicrobial agents in combating the rising AMR across the world after evaluating their cytotoxicity tests on animal models and clinical studies.

Conclusion

The synthesis of zinc molybdenum thiovanadate NPs was successfully achieved using a modified solvothermal technique. Comprehensive structural and morphological analyses confirmed the formation of a well-crystallized material with a uniform nanoscale morphology, demonstrating the reliability and reproducibility of the adopted synthesis procedure. The bioactivity assessment of the prepared NPs against three predominant waterborne bacterial strains demonstrated remarkable antibacterial performance, confirming their potential as efficient antimicrobial agents.

The promising bioactivity of these NPs can be attributed to the synergistic interaction among zinc, molybdenum, and vanadium ions, which enhances the generation of reactive oxygen species and disrupts bacterial cell membranes. Although this finding warrants deeper investigation, it suggests the potential of zinc molybdenum thiovanadate as a multifunctional nanomaterial for water purification, environmental remediation, and biomedical applications.

Future investigations should focus on elucidating the detailed antibacterial mechanism, evaluating the cytotoxicity toward human cells, and optimizing experimental parameters to further enhance performance and optimize their use in practical environmental and biomedical applications. Overall, zinc molybdenum thiovanadate NPs are introduced as a new and effective nanomaterial for antimicrobial technology to prevent waterborne bacterial diseases.

This study highlights the potential of exploratory synthesis of mixed metal sulfides as prospective candidates for nanomedicine applications. The findings can lead to the development of effective infection control and therapeutic strategies.

Conflicts of interest

There are no conflicts of interest to declare.

Data availability

The raw data supporting the conclusions of this article will be made available by the author on request.

Acknowledgements

The author is thankful to Dr Suriya Rehman, Department of Epidemic Diseases Research, Institute for Research and Medical Consultations (IRMC), Imam Abdulrahman Bin Faisal University, for assisting with the antimicrobial assay.

References

1 N. Baig, I. Kammakakam and W. Falath, Nanomaterials: a review of synthesis methods, properties, recent progress, and challenges, *Mater. Adv.*, 2021, **2**(6), 1821–1871.

2 F. Jamal, A. Rafique, S. Moeen, J. Haider, W. Nabgan, A. Haider, M. Imran, G. Nazir, M. Alhassan, M. Ikram, Q. Khan, G. Ali, M. Khan, W. Ahmad and M. Maqbool, Review of Metal Sulfide Nanostructures and their Applications, *ACS Appl. Nano Mater.*, 2023, **6**(9), 7077–7106.

3 C.-H. Lai, M.-Y. Lu and L.-J. Chen, Metal sulfide nanostructures: synthesis, properties and applications in energy conversion and storage, *J. Mater. Chem.*, 2012, **22**(1), 19–30.

4 H. Tang, L. N. Sacco, S. Vollebregt, H. Ye, X. Fan and G. Zhang, Recent advances in 2D/nanostructured metal sulfide-based gas sensors: mechanisms, applications, and perspectives, *J. Mater. Chem. A*, 2020, **8**(47), 24943–24976.

5 Z. A. Sandhu, M. A. Raza, U. Farwa, S. Nasr, I. S. Yahia, S. Fatima, M. Munawar, Y. Hadayet, S. Ashraf and H. Ashraf, Response surface methodology: a powerful tool for optimizing the synthesis of metal sulfide nanoparticles for dye degradation, *Mater. Adv.*, 2023, **4**(21), 5094–5125.

6 S. Ragu Nandhakumar, S. Rajeshkumar, R. S. Anand, V. Malyla, K. Dua, D. Ezhilarasan and T. Lakshmi, Chapter 20–Biogenic metal sulfide nanoparticles synthesis and applications for biomedical and environmental technology, in *Agri-Waste and Microbes for Production of Sustainable Nanomaterials*, ed, K. A. Abd-Elsalam, R. Periakaruppan and S. Rajeshkumar, Elsevier, 2022, pp. 495–506.

7 A. Shetty, H. Lang and S. Chandra, Metal Sulfide Nanoparticles for Imaging and Phototherapeutic Applications, *Molecules*, 2023, **28**(6), 2553.

8 W. Fei, M. Zhang, X. Fan, Y. Ye, M. Zhao, C. Zheng, Y. Li and X. Zheng, Engineering of bioactive metal sulfide nanomaterials for cancer therapy, *J. Nanobiotechnol.*, 2021, **19**(1), 93.

9 H. Labiadh, K. Lahbib, S. Hidouri, S. Touil and T. B. E. N. Chaabane, Insight of ZnS nanoparticles contribution in different biological uses, *Asian Pac. J. Trop. Med.*, 2016, **9**(8), 757–762.

10 S. Vijayan, C. S. Dash, G. Umadevi, M. Sundararajan and R. Mariappan, Investigation of Structural, Optical and Antibacterial Activity of ZnS Nanoparticles, *J. Clust. Sci.*, 2021, **32**(6), 1601–1608.

11 Y. Zhou, T. Tong, X. Jiang, L. Fang, Y. Wu, J. Liang and S. Xiao, GSH-ZnS Nanoparticles Exhibit High-Efficiency and Broad-Spectrum Antiviral Activities *via* Multistep Inhibition Mechanisms, *ACS Appl. Bio Mater.*, 2020, **3**(8), 4809–4819.

12 M. Abniki, Z. Azizi and H. A. Panahi, Design of 3-aminophenol-grafted polymer-modified zinc sulphide nanoparticles as drug delivery system, *IET Nanobiotechnol.*, 2021, **15**(8), 664–673.

13 A. A. P. Mansur, H. S. Mansur, S. M. Carvalho, Z. I. P. Lobato, M. d. F. Leite and L. L. Mansur, Fluorescent ZnS Quantum Dots–Phosphoethanolamine Nanoconjugates for Bioimaging Live Cells in Cancer Research, *ACS Omega*, 2018, **3**(11), 15679–15691.

14 O. Samy, S. Zeng, M. D. Birowosuto and A. El Moutaouakil, A Review on MoS_2 Properties, Synthesis, Sensing Applications and Challenges, *Crystals*, 2021, **11**(4), 355.

15 R. Wu, M. Dong and L. Liu, Nano–Bio Interface of Molybdenum Disulfide for Biological Applications, *Coatings*, 2023, **13**(6), 1122.

16 J. Lu, M. Chen, L. Dong, L. Cai, M. Zhao, Q. Wang and J. Li, Molybdenum disulfide nanosheets: From exfoliation preparation to biosensing and cancer therapy applications, *Colloids Surf., B*, 2020, **194**, 111162.

17 J. Wang, L. Sui, J. Huang, L. Miao, Y. Nie, K. Wang, Z. Yang, Q. Huang, X. Gong, Y. Nan and K. Ai, MoS_2-based nanocomposites for cancer diagnosis and therapy, *Bioact. Mater.*, 2021, **6**(11), 4209–4242.

18 X. Zhang, J. Wu, G. R. Williams, S. Niu, Q. Qian and L.-M. Zhu, Functionalized MoS_2-nanosheets for targeted drug delivery and chemo-photothermal therapy, *Colloids Surf., B*, 2019, **173**, 101–108.

19 J. Liu, K. Lu, F. Gao, L. Zhao, H. Li and Y. Jiang, Multifunctional MoS_2 composite nanomaterials for drug delivery and synergistic photothermal therapy in cancer treatment, *Ceram. Int.*, 2022, **48**(15), 22378–22386.

20 W. Yin, L. Yan, J. Yu, G. Tian, L. Zhou, X. Zheng, X. Zhang, Y. Yong, J. Li, Z. Gu and Y. Zhao, High-Throughput Synthesis of Single-Layer MoS_2 Nanosheets as a Near-Infrared Photothermal-Triggered Drug Delivery for Effective Cancer Therapy, *ACS Nano*, 2014, **8**(7), 6922–6933.

21 J. Liu, J. Zheng, H. Nie, H. Chen, B. Li and L. Jia, Co-delivery of erlotinib and doxorubicin by MoS_2 nanosheets for synergetic photothermal chemotherapy of cancer, *Chem. Eng. J.*, 2020, **381**, 122541.

22 M. Shi, L. Dong, S. Zheng, P. Hou, L. Cai, M. Zhao, X. Zhang, Q. Wang, J. Li and K. Xu, "Bottom-up" preparation of MoS_2 quantum dots for tumor imaging and their *in vivo* behavior study, *Biochem. Biophys. Res. Commun.*, 2019, **516**(4), 1090–1096.

23 V. Yadav, S. Roy, P. Singh, Z. Khan and A. Jaiswal, 2D MoS_2-Based Nanomaterials for Therapeutic, Bioimaging, and Biosensing Applications, *Small*, 2019, **15**(1), 1803706.

24 Y. Dong, J. Huo, C. Xu, D. Ji, H. Zhao, L. Li and Y. Lei, Research Progress on Vanadium Sulfide Anode Materials for Sodium and Potassium-Ion Batteries, *Adv. Mater. Technol.*, 2024, **9**(11), 2301840.

25 Y.-Y. Liu, L. Xu, X.-T. Guo, T.-T. Lv and H. Pang, Vanadium sulfide based materials: synthesis, energy storage and conversion, *J. Mater. Chem. A*, 2020, **8**(40), 20781–20802.

26 Z. Pei, H. Lei, J. Wu, W. Tang, K. Wei, L. Wang, F. Gong, N. Yang, L. Liu, Y. Yang and L. Cheng, Bioactive Vanadium

Disulfide Nanostructure with "Dual" Antitumor Effects of Vanadate and Gas for Immune-Checkpoint Blockade-Enhanced Cancer Immunotherapy, *ACS Nano*, 2023, **17**(17), 17105–17121.

27 S. Treviño, A. Díaz, E. Sánchez-Lara, B. L. Sanchez-Gaytan, J. M. Perez-Aguilar and E. González-Vergara, Vanadium in Biological Action: Chemical, Pharmacological Aspects, and Metabolic Implications in Diabetes Mellitus, *Biol. Trace Elem. Res.*, 2019, **188**(1), 68–98.

28 A. Ścibior, Ł. Pietrzyk, Z. Plewa and A. Skiba, Vanadium: Risks and possible benefits in the light of a comprehensive overview of its pharmacotoxicological mechanisms and multi-applications with a summary of further research trends, *J. Trace Elem. Med. Biol.*, 2020, **61**, 126508.

29 D. Rehder, The role of vanadium in biology, *Metallomics*, 2015, **7**(5), 730–742.

30 J. Liu, D. Wu, N. Zhu, Y. Wu and G. Li, Antibacterial mechanisms and applications of metal-organic frameworks and their derived nanomaterials, *Trends Food Sci. Technol.*, 2021, **109**, 413–434.

31 M. Farrukh, A. Munawar, Z. Nawaz, N. Hussain, A. B. Hafeez and P. Szweda, Antibiotic resistance and preventive strategies in foodborne pathogenic bacteria: a comprehensive review, *Food Sci. Biotechnol.*, 2025, **34**(10), 2101–2129.

32 I. Saba, K. Wani, K. M. Batoo, S. Rehman and S. Hameed, Carbon Nanomaterials as Antimicrobial Agents to Combat Multidrug Resistance, in *Nanotechnology Based Strategies for Combating Antimicrobial Resistance*, ed. M. Y. Wani, I. A. Waniand A. Rai, Springer Nature Singapore, Singapore, 2024, pp. 231–250.

33 K. Gyasi-Darko, A. D. Amofah, D. Ugwu, J. Apaflo and E. Oware, Initiatives to promote the responsible use of antibiotics and the development of new antimicrobial agents, *World J. Adv. Res. Rev.*, 2024, **24**, 2187–2194.

34 Y. Zhao, Z. Zhang, Z. Pan and Y. Liu, Advanced bioactive nanomaterials for biomedical applications, *Exploration*, 2021, **1**(3), 20210089.

35 P. Chowdhury, A. Roy and S. Ghosh, Molybdenum Disulfide Nanomaterials for Generating or Depleting Reactive Oxygen Species: Recent Development and Prospects in Biomedical Applications, *Small*, 2025, **21**(38), e06450.

36 J. P. Adamus, A. Ruszczyńska and A. Wyczałkowska-Tomasik, Molybdenum's Role as an Essential Element in Enzymes Catabolizing Redox Reactions: A Review, *Biomolecules*, 2024, **14**(7), 869.

37 R. Dinda, E. Garribba, D. Sanna, D. C. Crans and J. Costa Pessoa, Hydrolysis, Ligand Exchange, and Redox Properties of Vanadium Compounds: Implications of Solution Transformation on Biological, Therapeutic, and Environmental Applications, *Chem. Rev.*, 2025, **125**(3), 1468–1603.

38 K. Hashmi, Satya, P. Mishra, E. Veg, T. Khan and S. Joshi, The Potentiality of Vanadium Complexes as Antibacterial Agents, *Eng. Proc.*, 2025, **87**(1), 91.

39 H. O. Hassani, M. Akouibaa, S. Rakass, M. Abboudi, B. El Bali, M. Lachkar and F. Al Wadaani, A simple and cost-effective new synthesis method of copper molybdate CuMoO4 nanoparticles and their catalytic performance, *J. Sci. Adv. Mater. Devices*, 2021, **6**(3), 501–507.

40 K. M. Koczkur, S. Mourdikoudis, L. Polavarapu and S. E. Skrabalak, Polyvinylpyrrolidone (PVP) in nanoparticle synthesis, *Dalton Trans.*, 2015, **44**(41), 17883–17905.

41 S. Rehman, V. Ravinayagam, S. S. Al-Jameel, S. Mehmood Ali, S. Z. Alzayer, Z. M. Alfaraj, A. Alboeid, N. Alamri, S. H. Al Isam, H. Dafallae, S. Dhanasekaran, G. Tanimu, F. Alam Khan and B. Rabindran Jermy, Controlling cisplatin release by synergistic action of silver-cisplatin on monodispersed spherical silica for targeted anticancer and antibacterial activities, *Arabian J. Chem.*, 2024, **17**(4), 105661.

42 J. Rodriguez-Carvajal, in *FULLPROF: a Program for Rietveld Refinement and Pattern Matching Analysis, Satellite Meeting on Powder Diffraction of the XV Congress of the IUCr*, Toulouse, France:[sn]: 1990.

43 J. Rodriguez-Carvajal, Recent developments of the program FULLPROF, commission on powder diffraction, *(IUCr) Newsletter*, 2001, **26**, 12–19.

44 A. L. Patterson, The Scherrer Formula for X-Ray Particle Size Determination, *Phys. Rev.*, 1939, **56**(10), 978–982.

45 A. C. Gimenez-Ingalaturre, E. Rubio, P. Chueca, F. Laborda and P. Goñi, Contribution to optimization and standardization of antibacterial assays with silver nanoparticles: the culture medium and their aggregation, *J. Microbiol. Methods*, 2022, **203**, 106618.

46 C. Zhang, Z. Wang, S. Bhoyate, T. Morey, B. L. Neria, V. Vasiraju, G. Gupta, S. Palchoudhury, P. K. Kahol, S. R. Mishra, F. Perez and R. K. Gupta, MoS_2 Decorated Carbon Nanofibers as Efficient and Durable Electrocatalyst for Hydrogen Evolution Reaction, *C*, 2017, **3**(4), 33.

47 C. Zhang, Z. Wang, S. Bhoyate, T. Morey, B. L. Neria, V. Vasiraju, G. Gupta, S. Palchoudhury, P. K. Kahol, S. R. Mishra, F. Perez and R. K. Gupta, MoS_2 Decorated Carbon Nanofibers as Efficient and Durable Electrocatalyst for Hydrogen Evolution Reaction, *C*, 2017, **3**(4), 33.

48 L. Mao, F. Wang and J. Mao, Polar mesoporous zinc sulfide nanosheets encapsulated in reduced graphene oxide three-dimensional foams for sulfur host, *Sci. Rep.*, 2020, **10**(1), 5256.

49 H. Cheng, Q. Liu, Y. Diao, L. Wei, J. Chen and F. Wang, CoMo2S4 with Superior Conductivity for Electrocatalytic Hydrogen Evolution: Elucidating the Key Role of Co, *Adv. Funct. Mater.*, 2021, **31**(37), 2103732.

50 X. Zhou, W. Zhao, J. Pan, Y. Fang, F. Wang and F. Huang, Urchin-like Mo2S3 prepared *via* a molten salt assisted method for efficient hydrogen evolution, *Chem. Commun.*, 2018, **54**(90), 12714–12717.

51 S. Rajagopal, D. Nataraj, O. Y. Khyzhun, Y. Djaoued, J. Robichaud, K. Senthil and D. Mangalaraj, Systematic synthesis and analysis of change in morphology, electronic structure and photoluminescence properties of pyrazine intercalated MoO_3 hybrid nanostructures, *CrystEngComm*, 2011, **13**(7), 2358–2368.

52 S. Cheng, K. Yao, K. Zheng, Q. Li, D. Chen, Y. Jiang, W. Liu, Y. Feng, X. Rui and Y. Yu, Self-Assembled VS

Hierarchitectures with Enhanced Capacity and Stability for Sodium Storage, *Energy Environ. Mater.*, 2022, **5**(2), 592–598.

53 S. Rehman, F. Alahmari, L. Aldossary, M. Alhout, S. S. Aljameel, S. M. Ali, J. S. M. Sabir, F. A. Khan and I. A. Rather, Nano-sized warriors: zinc chromium vanadate nanoparticles as a dual solution for eradicating waterborne enterobacteriaceae and fighting cancer, *Front. Pharmacol.*, 2023, **14**, 1213824.

54 M. Narayanasamy, B. Balan, C. Yan and S. Angaiah, Cauliflower-like nanostructured ZnV_2S_4 as a potential cathode material to boost-up high capacity and durability of the aqueous zinc-ion battery, *Chin. Chem. Lett.*, 2023, **34**(8), 108076.

55 L. Chen, J. Ma, M. Wang, W. Dai, Y. Zhou, G. Li, Q. Li, Y. Feng, J. Li, B. Zou and X. Li, Electrochemical dynamic regulation of in-situ copper ion doped CoV_2S_4 nanohollow cubic boxes for fast electrochemical activation and high efficient sodium ion storage, *J. Alloys Compd.*, 2025, **1018**, 179087.

56 Z. Ibupoto, K. Khun, X. Liu and M. Willander, Hydrothermal Synthesis of Nanoclusters of ZnS Comprised on Nanowires, *Nanomaterials*, 2013, **3**, 564–571.

57 A. Empel, E. Kisiel, R. D. Wojtyczka, M. Kępa, D. Idzik, A. Sochanik, T. J. Wąsik and A. Zięba, Synthesis and Antimicrobial Activity of Sulfur Derivatives of Quinolinium Salts, *Molecules*, 2018, **23**(1), 218.

58 C. Marambio-Jones and E. M. V. Hoek, A review of the antibacterial effects of silver nanomaterials and potential implications for human health and the environment, *J. Nanopart. Res.*, 2010, **12**(5), 1531–1551.

59 S. Rehman, V. Ravinayagam, S. Al-Jammel, S. Ali, S. Alzayer, Z. Alfaraj, A. Alboeid, N. Alamri, S. Isam, H. Dafallae, S. Dhanasekaran, G. Tanimu, F. A. Khan and R. Jermy, Controlling Cisplatin Release by Synergistic Action of Silver-Cisplatin on Monodispersed Spherical Silica for Targeted Anticancer and Antibacterial Activities, *Arabian J. Chem.*, 2024, **17**, 105661.

60 P. V. AshaRani, G. Low Kah Mun, M. P. Hande and S. Valiyaveettil, Cytotoxicity and Genotoxicity of Silver Nanoparticles in Human Cells, *ACS Nano*, 2009, **3**(2), 279–290.

61 N. Basavegowda and K. H. Baek, Multimetallic Nanoparticles as Alternative Antimicrobial Agents: Challenges and Perspectives, *Molecules*, 2021, **26**(4), 912.

62 P. Kalakonda, P. Mandal, S. Mynepally, A. Bashipangu, A. Kethavath, S. Khanam, M. Batchu, P. B. Kalakonda, S. Banne, D. Aitipamula, M. Banavoth, M. Kigoji, V. Shukla, Y. Eluri and B. Podila, Comparison of Multi-metallic Nanoparticles-Alternative Antibacterial Agent: Understanding the Role of Their Antibacterial Properties, *J. Inorg. Organomet. Polym. Mater.*, 2024, **34**, 1–16.

63 L. Wang, C. Hu and L. Shao, The antimicrobial activity of nanoparticles: present situation and prospects for the future, *Int. J. Nanomed.*, 2017, **12**, 1227–1249.

64 M. J. Hajipour, K. M. Fromm, A. A. Ashkarran, D. Jimenez de Aberasturi, I. R. de Larramendi, T. Rojo, V. Serpooshan, W. J. Parak and M. Mahmoudi, Antibacterial properties of nanoparticles, *Trends Biotechnol.*, 2012, **30**(10), 499–511.